

Water ^1H Magnetic Relaxation Dispersion in Protein Solutions. A Quantitative Assessment of Internal Hydration, Proton Exchange, and Cross-Relaxation

Kandadai Venu,^{*,†} Vladimir P. Denisov,^{*} and Bertil Halle^{*}

Contribution from the Condensed Matter Magnetic Resonance Group, Department of Chemistry, Lund University, P.O. Box 124, S-22100 Lund, Sweden

Received October 16, 1996[⊗]

Abstract: The dispersion of the water ^1H longitudinal relaxation rate in the frequency range 2–100 MHz has been measured in aqueous solutions of bovine pancreatic trypsin inhibitor (BPTI) and a mutant protein (G36S) lacking one of the four internal water molecules. The ^1H relaxation dispersion has also been measured for BPTI in a series of $\text{H}_2\text{O}/\text{D}_2\text{O}$ mixtures. The quantitative analysis of these data resolve the major controversies in the interpretation of water ^1H relaxation data from protein solutions and has implications for medical magnetic resonance imaging. Three principal conclusions are drawn. First, as previously found for the water ^2H and ^{17}O dispersions, the BPTI – G36S difference ^1H dispersion can be quantitatively accounted for by a single, fully ordered, internal water molecule (W122). The intrinsic relaxation rate of these water protons is *ca.* 70% intramolecular, with the intramolecular dipole coupling constant as in ice, and *ca.* 30% intermolecular, with significant dipole couplings to many BPTI protons. Second, exchanging protons in the protein make a substantial contribution to the observed water ^1H relaxation rate. This contribution should be dominant even at neutral pH for most proteins. Third, the effect of intermolecular dipole couplings with protein protons is additive, and cross-relaxation effects are negligible. A theoretical analysis of dipole relaxation in a multispin system undergoing chemical exchange with an abundant bulk phase shows that this conclusion holds generally within the regime of motional narrowing theory.

Introduction

Since the pioneering study by Daszkiewicz *et al.* in 1963,¹ proton relaxation studies of water–protein interactions and dynamics have grown into an active field of investigation. While such studies have always been of fundamental biophysical interest, they are now also motivated by the importance of relaxation-based contrast in clinical applications of magnetic resonance imaging. It was recognized at an early stage^{2–4} that the frequency dependence of the longitudinal relaxation rate, the nuclear magnetic relaxation dispersion (NMRD), contains information about water–protein interactions and dynamics. Extracting this information turned out to be nontrivial, however, and after nearly three decades of ^1H NMRD studies of protein solutions and other biological systems a consensus view is still lacking.^{5–8} The interpretational controversy concerns three major issues: (i) the nature of the protein-associated water that contributes to the relaxation dispersion: its location, orientational order, and residence time, (ii) the relative importance of direct contributions to the observed ^1H relaxation rate from labile protein protons exchanging with water, and (iii) the effect of

cross-relaxation between the longitudinal magnetizations associated with water protons and protein protons.

The principal obstacle to progress in the water NMRD field has been the difficulty of establishing the molecular mechanism whereby hydration water senses the rotational diffusion of the protein. This mechanism has only recently been identified by ^2H and ^{17}O NMRD studies of several proteins.^{9–15} These studies unambiguously demonstrate that the ^{17}O relaxation dispersion is due neither to a long-range hydrodynamic effect as argued for 15 years^{5,16} nor to long-lived water molecules at the protein surface as currently advocated by several workers^{7,17–19} but to a small number of crystallographically well-defined water molecules buried inside the protein and exchanging with bulk water on a submicrosecond time scale. The ^2H dispersion generally includes an additional contribution from labile protein hydrogens.¹¹ Since the intrinsic ^1H relaxation times of labile protons are 1–2 orders of magnitude longer than the ^2H rates, the labile proton contribution to the ^1H dispersion should be correspondingly larger, possibly dominating over the hydration water contribution. This is probably the main reason why ^1H

[†] Permanent address: School of Physics, University of Hyderabad, Hyderabad – 500046, India.

[⊗] Abstract published in *Advance ACS Abstracts*, March 1, 1997.

(1) Daszkiewicz, O. K.; Hennel, J. W.; Lubas, B.; Szczepkowski, T. W. *Nature* **1963**, *200*, 1006–1007.

(2) Koenig, S. H.; Schillinger, W. E. *J. Biol. Chem.* **1969**, *244*, 3283–3289.

(3) Kimmich, R.; Noack, F. Z. *Naturforsch.* **1970**, *25a*, 299–301, 1680–1684.

(4) Blicharska, B.; Florkowski, Z.; Hennel, J. W.; Held, G.; Noack, F. *Biochim. Biophys. Acta* **1970**, *207*, 381–389.

(5) Koenig, S. H.; Brown, R. D. *Progr. NMR Spectrosc.* **1991**, *22*, 487–567.

(6) Belton, P. S. *Prog. Biophys. Molec. Biol.* **1994**, *61*, 61–79.

(7) Koenig, S. H. In *Encyclopedia of Nuclear Magnetic Resonance*; Grant, D. M., Harris, R. K., Eds.; Wiley: New York, 1995; pp 1819–1830.

(8) Bryant, R. G. *Annu. Rev. Biophys. Biomol. Struct.* **1996**, *25*, 29–53.

(9) Denisov, V. P.; Halle, B. *J. Am. Chem. Soc.* **1994**, *116*, 10324–10325.

(10) Denisov, V. P.; Halle, B. *J. Mol. Biol.* **1995**, *245*, 682–697.

(11) Denisov, V. P.; Halle, B. *J. Mol. Biol.* **1995**, *245*, 698–709.

(12) Denisov, V. P.; Halle, B. *J. Am. Chem. Soc.* **1995**, *117*, 8456–8465.

(13) Denisov, V. P.; Halle, B.; Peters, J.; Hörlein, H. D. *Biochemistry* **1995**, *34*, 9046–9051.

(14) Denisov, V. P.; Peters, J.; Hörlein, H. D.; Halle, B. *Nature Struct. Biol.* **1996**, *3*, 505–509.

(15) Denisov, V. P.; Halle, B. *Faraday Discuss.* **1997**, *103*, in press.

(16) Koenig, S. H.; Hallenga, K.; Shporer, M. *Proc. Natl. Acad. Sci. U.S.A.* **1975**, *72*, 2667–2671.

(17) Kimmich, R.; Gneiting, T.; Kotitschke, K.; Schnur, G. *Biophys. J.* **1990**, *58*, 1183–1197.

(18) Koenig, S. H.; Brown, R. D.; Ugolini, R. *Magn. Reson. Med.* **1993**, *29*, 77–83.

(19) Koenig, S. H. *Biophys. J.* **1995**, *69*, 593–603.

NMRD studies failed to identify the mechanism behind the hydration water dispersion.

We report here new ^1H NMRD data from solutions of bovine pancreatic trypsin inhibitor (BPTI), perhaps the best understood of all globular proteins. Results from two types of NMRD experiments are presented. The first is a difference NMRD experiment, where wild-type BPTI is compared with the G36S mutant of BPTI, lacking one of the four internal water molecules.²⁰ The difference dispersion profile thus monitors the relaxation enhancement produced by a single internal water molecule (denoted W122). We have recently used this approach with the quadrupolar water nuclei ^2H and ^{17}O , establishing that W122 is fully ordered and exchanges with a residence time of $170 \pm 20 \mu\text{s}$ at 27°C .^{13,14} In the second experiment, we record the ^1H NMRD profiles from a series of BPTI solutions differing only in the H/D isotopic composition of the solvent. Such isotope dilution experiments can be used to isolate the contribution to the ^1H relaxation rate from intermolecular dipole couplings with nonexchangeable protein protons.^{4,21–26}

Besides the detailed information available from recent ^2H and ^{17}O NMRD studies,^{9–14} two additional circumstances combine to make BPTI an ideal protein for disentangling the complex interplay of water and proton exchange and of intra- and intermolecular dipole couplings that influence the ^1H relaxation rate. First, a high-resolution crystal structure is available, based on jointly refined neutron and X-ray diffraction data, providing the spatial coordinates of all protons, including those of the four internal water molecules.²⁷ This geometrical information makes it possible to calculate the intermolecular contributions to the dipole relaxation of internal water protons and labile BPTI protons. Second, most of the exchange rate constants for the labile protons of BPTI are known,^{11,28,29} permitting reliable estimates of the direct labile proton contribution to ^1H relaxation at any pH.

Drawing on the massive body of information about BPTI, including the recent ^2H and ^{17}O NMRD results,^{9–14} we are able to quantitatively rationalize the new ^1H NMRD data, thereby resolving the three major interpretational ambiguities mentioned above. Taking into account a 30% intermolecular contribution, calculated from crystal structure data, and using the ice value for the intramolecular dipole coupling constant of H_2O , we thus obtain quantitative agreement with the ^2H and ^{17}O results for the isolated internal water molecule W122. A similar agreement is found for the other three internal water molecules. The direct contribution from labile BPTI protons is comparable to that from one internal water molecule at pH 5.1 but dominates the ^1H dispersion at pH 7. This is an important result, since the labile proton contribution has frequently been assumed negligible at neutral pH.^{5,7,8,16–18,22,26,30,31} Finally, the present finding that the ^1H relaxation dispersion can be quantitatively rationalized without invoking cross-relaxation indicates that magnetization

transfer between water and protein protons does not significantly affect the observed water ^1H relaxation. This conclusion is corroborated here by a rigorous theoretical analysis of dipole relaxation in an exchanging multispin system, showing that, for BPTI, the cross-relaxation effect is within the experimental uncertainty of *ca.* 1% in the measured relaxation rate.

The dynamical coupling of water and protein proton polarizations *via* an intermolecular dipole interaction is well understood theoretically^{32,33} and provides the basis for studies of protein hydration through the nuclear Overhauser effect (NOE) in saturation transfer experiments^{34–38} and in two-dimensional NOE spectroscopy.^{39,40} Since the nature of the dynamical water–protein coupling underlying the ^1H dispersion was not known, however, cross-relaxation in the context of water ^1H NMRD has traditionally been described by phenomenological models based on solid-state concepts such as spin temperature and spin diffusion,^{5,22,41–43} of doubtful validity for protein solutions. Since the phenomenological model of cross-relaxation is mathematically isomorphic with the formalism of two-state chemical exchange⁴⁴ and since it involves parameters of obscure physical significance, it is not easily confirmed or refuted by experimental data. Nevertheless, cross-relaxation has frequently been invoked to interpret water ^1H relaxation data from protein solutions.^{3,5,7,22,24,26,45–48} The present more rigorous theoretical analysis shows, however, that the effect of cross-relaxation is negligible, a result consistent with the experimental data presented here. Furthermore, we argue that this conclusion holds generally within the regime of the conventional motional narrowing theory of spin relaxation. The main arguments for the importance of cross-relaxation have come from isotope dilution experiments and comparisons of ^1H and ^2H NMRD profiles. Here we compare for the first time the NMRD profiles of all three water nuclei (^1H , ^2H , and ^{17}O) and find that the differences between them can be quantitatively accounted for in terms of exchanging internal water molecules and labile protons and an additive intermolecular auto-relaxation contribution. There is thus no need to invoke cross-relaxation. The same conclusion emerges from the analysis of the isotope dilution experiment.

Materials and Methods

Protein Solutions. Recombinant bovine pancreatic trypsin inhibitor (BPTI) and the G36S mutant were obtained from Bayer AG, Wuppertal, Germany. The preparation of the mutant protein has been described.²⁰ Wild-type and mutant proteins were subjected to the same purification

(20) Berndt, K. D.; Beunink, J.; Schröder, W.; Wüthrich, K. *Biochemistry* **1993**, *32*, 4564–4570.

(21) Hilton, B. D.; Bryant, R. G. *J. Magn. Reson.* **1976**, *21*, 105–108.
(22) Koenig, S. H.; Bryant, R. G.; Hallenga, K.; Jacob, G. S. *Biochemistry* **1978**, *17*, 4348–4358.

(23) Rydzy, M.; Skrzynski, W. *Biochim. Biophys. Acta* **1982**, *705*, 33–37.

(24) Eisenstadt, M. *Biochemistry* **1985**, *24*, 3407.

(25) Conti, S. *Molec. Phys.* **1986**, *59*, 449–482.

(26) Prosser, S.; Peemoeller, H. *Biochem. Cell Biol.* **1991**, *69*, 341–345.

(27) Wlodawer, A.; Walter, J.; Huber, R.; Sjölin, L. *J. Mol. Biol.* **1984**, *180*, 301–329.

(28) Tüchsen, E.; Woodward, C. *J. Mol. Biol.* **1985**, *185*, 405–419.

(29) Liepinsh, E.; Otting, G.; Wüthrich, K. *J. Biomol. NMR* **1992**, *2*, 447–465.

(30) Hallenga, K.; Koenig, S. H. *Biochemistry* **1976**, *15*, 4255–4264.

(31) Bryant, R. G.; Jarvis, M. *J. Phys. Chem.* **1984**, *88*, 1323–1324.

(32) Solomon, I. *Phys. Rev.* **1955**, *99*, 559–565.

(33) Noggle, J. H.; Schirmer, R. E. *The Nuclear Overhauser Effect*; Academic Press: New York, 1971.

(34) Stoesz, J. D.; Redfield, A. G.; Malinowski, D. *FEBS Lett.* **1978**, *91*, 320–324.

(35) Akasaka, K. *J. Magn. Reson.* **1979**, *36*, 135–140.

(36) Wolff, S. D.; Balaban, R. S. *Magn. Reson. Med.* **1989**, *10*, 135–144.

(37) Grad, J.; Bryant, R. G. *J. Magn. Reson.* **1990**, *90*, 1–8.

(38) Iino, M. *Biochim. Biophys. Acta* **1994**, *1208*, 81–88.

(39) Otting, G.; Wüthrich, K. *J. Am. Chem. Soc.* **1989**, *111*, 1871–1875.

(40) Otting, G.; Liepinsh, E. *Acc. Chem. Res.* **1995**, *28*, 171–177.

(41) Edzes, H. T.; Samulski, E. T. *J. Magn. Reson.* **1978**, *31*, 207–229.

(42) Hills, B. P. *Molec. Phys.* **1992**, *76*, 489–508.

(43) Lester, C. C.; Bryant, R. G. *Magn. Reson. Med.* **1991**, *22*, 143–153.

(44) Zimmerman, J. R.; Brittin, W. E. *J. Phys. Chem.* **1957**, *61*, 1328–1333.

(45) Kimmich, R.; Noack, F. *Ber. Bunsenges. Phys. Chem.* **1971**, *75*, 269–272.

(46) Eley, D. D.; Hey, M. J.; Ward, A. J. I. *J. Chem. Soc., Faraday Trans. 1* **1975**, *71*, 1106–1113.

(47) Grösch, L.; Noack, F. *Biochim. Biophys. Acta* **1976**, *453*, 218–232.

(48) Eisenstadt, M.; Fabry, M. E. *J. Magn. Reson.* **1978**, *29*, 591–597.

steps and were lyophilized as salts of trifluoroacetic acid. The purity of both protein preparations was 99.7% according to SDS-PAGE and RP-HPLC.

Protein solutions were made by dissolving the lyophilized proteins in doubly distilled water. A small amount of 5 M NaOH was added to the protein solutions to give pH 5.1. The protein concentrations in the NMR samples were determined by complete amino acid analysis to 16.75 mM (wild-type) and 16.50 mM (mutant). The former concentration corresponds to a water/BPTI mol ratio, $N_T = 3045$.

The H/D isotope dilution experiment was carried out with recombinant BPTI (Aprotinin, batch no. A46R02) of 99.5% purity from Novo Nordisk A/S, Gentofte, Denmark. Four protein solutions were made by dissolving the lyophilized protein in H₂O/D₂O mixtures of different isotopic composition. D₂O of >99.8 atom % D was obtained from Glaser AG, Basel, Switzerland. The deuterium atom fraction x in the exchanging hydrogen pool (water and labile BPTI hydrogens) was calculated from the gravimetric sample composition, making a small correction for protons originating from H₂O in the lyophilized protein (87% BPTI according to amino acid analysis) and from labile BPTI groups. The BPTI concentration was 18.9 mM ($N_T = 2600$), differing by less than 1% among the four samples. All solutions had pL = 5.1, where pL = pH* + 0.4 x and pH* is the uncorrected meter reading in an isotopically mixed solvent.

Relaxation Dispersion Measurements. The longitudinal relaxation rate, R_1 , of the water proton magnetization was measured with nonselective inversion recovery using essentially the same protocol as for ²H and ¹⁷O.^{10,11} For the delay times used ($\tau > 0.05T_1$), no significant deviations from single-exponential magnetization recovery could be detected. No attempts were made to observe the initial fast relaxation of the magnetization associated with nonexchanging BPTI protons.^{23,26} The relaxation dispersion comprised 16 magnetic field strengths, corresponding to ¹H Larmor frequencies in the range 2.25–100 MHz. Up to 80 MHz, the measurements were performed with a Bruker MSL 100 spectrometer equipped with an iron magnet (Drusch EAR-35N) with field-variable lock and flux stabilizer. For the highest field, a Bruker DMX 100 spectrometer was used. The sample temperature was maintained at 27.0 ± 0.1 °C by a thermostated air flow and a Stellar VTC87 temperature regulator unit.

Prior to relaxation measurements, the samples (1.35 or 0.30 mL in 10 or 5 mm NMR tubes thoroughly rinsed with 3 M HCl and EDTA solutions) were gently bubbled by argon gas for 2–4 h. This procedure virtually eliminated the small paramagnetic contribution, from dissolved oxygen, to the proton relaxation rate.⁴⁹ A pure water reference sample treated in this way gave $R_{\text{bulk}} = 0.274 \text{ s}^{-1}$, with no significant frequency dependence in the investigated range. The standard literature value⁵⁰ is $R_{\text{bulk}} = 0.265 \text{ s}^{-1}$. The accuracy of the reported relaxation rates is estimated to ca. 1%, except at the two lowest fields. Due to the slight concentration difference between the wild-type and mutant protein solutions, the mutant data were corrected to the wild-type concentration according to $R_1(\text{G36S, corrected}) = R_{\text{bulk}} + (R_1(\text{G36S}) - R_{\text{bulk}})c(\text{WT})/c(\text{G36S})$. This correction was always less than 1%.

Results and Discussion

Proton Relaxation Dispersions from BPTI and G36S. The longitudinal relaxation dispersion of the water proton resonance in solutions of wild-type (WT) and mutant (G36S) BPTI are shown in Figure 1. As observed for the corresponding water ²H and ¹⁷O dispersions,^{13,14} the magnitude of the dispersion step is distinctly smaller for the mutant. The two proteins have virtually identical structure, except for the replacement of the deeply buried water molecule W122 in wild-type BPTI by the hydroxyl group of the serine–36 side-chain in the G36S mutant.²⁰ As in the case of the ²H and ¹⁷O dispersions,^{13,14} the difference between the ¹H dispersions, shown directly in Figure 2, can therefore be ascribed to the single internal water molecule W122.

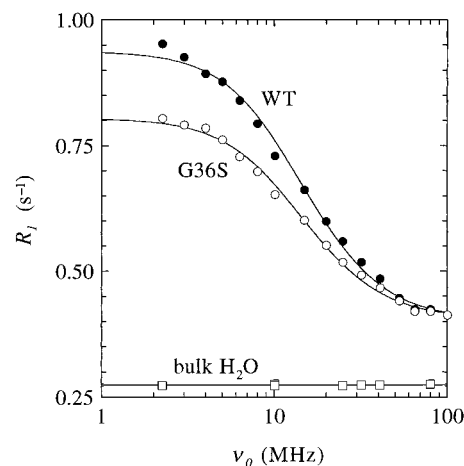


Figure 1. Dispersion of the water ¹H longitudinal relaxation rate in solutions of wild-type (WT) and mutant (G36S) BPTI at 27.0 °C, pH 5.1, and 16.75 mM protein concentration. The curves resulted from three-parameter fits according to eq 1. Data from a pure water reference sample are also shown, with the line representing the average value. Except for the two lowest frequencies, the estimated error bars (ca. 1%) are roughly the same size as the data symbols.

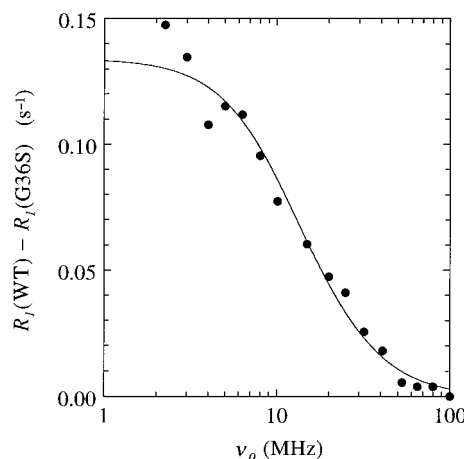


Figure 2. The difference of the WT and G36S dispersion data in Figure 1, reflecting the single internal water molecule W122. The curve resulted from a two-parameter fit according to eq 1 with $\alpha = 0$.

The curves shown in Figure 1 were obtained by adjusting the three parameters α , β , and τ_c in the relaxation dispersion relation^{10,15}

$$R_1(\omega_0) = R_{\text{bulk}} + \alpha + \beta\tau_c \left(\frac{0.2}{1 + (\omega_0\tau_c)^2} + \frac{0.8}{1 + (2\omega_0\tau_c)^2} \right) \quad (1)$$

This dispersion relation is strictly valid only for an isolated pair of dipole-coupled equivalent $I = 1/2$ nuclei or for $I = 1$ nuclei interacting with an electric field gradient.⁵¹ Although we shall show that the ¹H dispersion has a substantial contribution from intermolecular dipole couplings to BPTI protons, it turns out that, to an excellent approximation, the functional form of eq 1 may be retained, provided that the parameters are interpreted appropriately.

Disregarding for the moment the intermolecular contribution as well as any contribution from labile BPTI protons, the parameter α characterizing the high-frequency relaxation rate plateau can be ascribed to N_S short-lived water molecules at the protein surface, while the parameter β characterizing the magnitude of the relaxation dispersion can be ascribed to N_I long-lived internal water molecules. If the latter have residence times, τ_I , much longer than the rotational correlation time, τ_R ,

(49) Hausser, R.; Noack, F. *Z. Naturforsch.* **1965**, *20a*, 1668–1675.

(50) Hindman, J. C.; Svirmickas, A.; Wood, M. J. *Chem. Phys.* **1973**, *59*, 1517–1522.

Table 1. Parameter Values Deduced from Fits of Eq 1 to the ^1H Relaxation Dispersion Data in Figures 1 and 2

data	α (s^{-1})	β (10^7 s^{-2})	τ_c (ns)
WT	0.130 ± 0.003	8.60 ± 0.17	6.2 ± 0.1
G36S	0.132 ± 0.003	6.42 ± 0.16	6.2 ± 0.2
difference		2.03 ± 0.13	6.6 ± 0.6

of the protein, we can make the identification $\tau_c = \tau_R$.¹⁵ In the absence of intermolecular dipole couplings, we then have^{10,15,51}

$$\alpha = (N_S/N_T)(\langle R_S \rangle - R_{\text{bulk}}) \quad (2)$$

$$\beta = (N_I/N_T) \frac{3}{2} (DA)^2 \quad (3)$$

where N_T is the total number of water molecules per protein molecule in the solution ($N_T = 3045$ here), A is a generalized orientational order parameter,^{12,52,53} and D is the intramolecular dipole coupling constant⁵¹

$$D = \left(\frac{\mu_0}{4\pi} \right) \frac{\hbar \gamma^2}{r_{HH}^3} \quad (4)$$

The parameter values deduced from the fits in Figures 1 and 2 are collected in Table 1. If, as previously shown,²⁰ the point mutation in G36S induces only local structural changes, we expect α (which depends on the average structure of the protein surface) and τ_c (which depends on the overall size and shape of the protein) to be unaffected. The data in Table 1 clearly confirm this expectation. In contrast, the parameter β , which depends on the number of long-lived internal water molecules, is significantly smaller for the G36S mutant, where one of the four internal water molecules has been expelled.²⁰ A direct two-parameter fit to the difference NMRD data (Figure 2) yields a value for β that does not differ significantly from the difference of the β values deduced from the WT and G36S fits (Figure 1).

Using eq 2 with $N_T = 3045$ and $R_{\text{bulk}} = 0.274 \text{ s}^{-1}$, we find that the α value in Table 1 corresponds to $N_S(\langle R_S \rangle / R_{\text{bulk}} - 1) = 1460 \pm 30$, in close agreement with the values 1380 ± 40 and 1460 ± 50 previously deduced from the ^2H and ^{17}O dispersions, respectively, from the same protein preparations.¹³ All these results are likely to be slightly high due to the presence of *ca.* 0.5 M trifluoroacetate in the protein solutions.¹³ Using instead the α value from the H_2O solution of BPTI used in the H/D isotope dilution experiment (*vide infra*), we obtain $N_S(\langle R_S \rangle / R_{\text{bulk}} - 1) = 1280 \pm 40$, close to the value 1200 ± 50 deduced from the ^2H and ^{17}O dispersion from this BPTI preparation.^{10,11} Taking $N_S = 230$ ¹⁰ and assuming that the bulk water coupling constants are unaffected, we find that these values correspond to a slowing down of the water dynamics at the protein surface by an average factor of 6–7 as compared to bulk water.

Although we focus in this study on the dispersion in the 1–100 MHz range, mention should be made of several potential complications in the interpretation of the high-frequency ^1H relaxation enhancement α . In general, α values derived from ^1H or ^2H dispersions include a contribution from labile hydrogens. For BPTI at pH 5, however, this contribution should be quite small, as previously demonstrated for ^2H .¹¹ Whereas the slower relaxation of ^1H (compared to ^2H) brings a larger number of labile protons into the fast exchange regime, the much slower relaxation of the dominant (at pH 5) hydroxyl protons

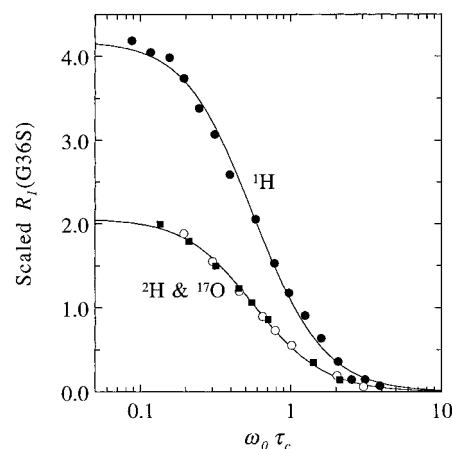


Figure 3. Dispersion of the water ^1H , ^2H , and ^{17}O longitudinal relaxation rates in solutions of the G36S mutant at 27.0 °C and pH 5.1 (^1H) or pH* 5.2 (^2H and ^{17}O). To allow a direct comparison, the data have been scaled as in eq 5. The curves resulted from three-parameter fits according to eq 1. The ^2H and ^{17}O data have been reported previously.¹³

(compared to water protons) decreases the relative contribution of labile hydrogens to α . Another complication is that the intermolecular relaxation contribution may differ for surface water and bulk water. The close agreement between the scaled α values from the three nuclei, however, indicates that both these complications are unimportant under the present conditions. We note also that, in principle, the high-frequency relaxation enhancement could be dominated by a small number of surface water molecules with effective correlation times around 0.3 ns, in which case a second dispersion step should appear above 100 MHz. However, such a scenario is not supported by relaxation data (not shown) on a different BPTI sample (14 wt %, pH 3.9 and 7.5, 4 °C), revealing no significant R_1 variation in the range 200–600 MHz.

The correlation time, $\tau_c = 6.2 \pm 0.2$ ns, obtained here for WT, and G36S BPTI can be identified with the rotational correlation time, τ_R , of the protein. Previous ^2H and ^{17}O studies¹³ of the same protein preparations but at somewhat higher concentrations (22.7 and 25.7 mM) than here (16.8 mM) gave $\tau_c = 8.4 \pm 0.2$ ns (^2H) and 6.6 ± 0.2 ns (^{17}O). At the lower concentration 5 mM, $\tau_c = 2.4 \pm 0.6$ ns has been obtained by ^{15}N relaxation.⁵⁴ The longer correlation times obtained at the higher protein concentrations can be ascribed to protein–protein interactions.^{10,55} All τ_c values quoted here, when not measured in H_2^{16}O at 300 K, have been scaled to $T = 300$ K and $\eta = 0.851$ cP, assuming $\tau_c \propto \eta/T$.

Comparison of ^1H , ^2H , and ^{17}O Dispersions. In the analysis of water relaxation dispersion data from protein solutions, comparisons of relaxation data from different water nuclei have played an important role.^{5,11–16,22,30,57} Previously, however, comparisons of complete NMRD profiles for a given protein have been limited to two of the three water nuclei; either the hydrogen isotopes ^1H and ^2H ^{5,16,22,30} or the quadrupolar nuclei ^2H and ^{17}O .^{11–15} Figure 3 presents, for the first time, the dispersion profiles of all three water nuclei in a protein solution, namely the G36S mutant of BPTI. The ^2H and ^{17}O data have been reported previously.¹³

(54) Szyperski, T.; Luginbühl, P.; Otting, G.; Güntert, P.; Wüthrich, K. *J. Biomol. NMR* **1993**, *3*, 151–164.

(55) Gallagher, W. H.; Woodward, C. K. *Biopolymers* **1989**, *28*, 2001–2024.

(56) Valensin, G.; Niccolai, N. *Chem. Phys. Lett.* **1981**, *79*, 47–50.

(57) Piculell, L.; Halle, B. *J. Chem. Soc., Faraday Trans 1* **1986**, *82*, 401–414.

(51) Abragam, A. *The Principles of Nuclear Magnetism*; Clarendon Press: Oxford, 1961.

(52) Halle, B.; Wennerström, H. *J. Chem. Phys.* **1981**, *75*, 1928–1943.

(53) Lipari, G.; Szabo, A. *J. Am. Chem. Soc.* **1982**, *104*, 4546–4559.

To enable a direct comparison of the different nuclei, the relaxation dispersion profiles are presented in reduced form, with the scaled relaxation rate defined as

$$R_1^{\text{scaled}} = (R_1 - \alpha - R_{\text{bulk}}) \frac{N_T}{C\tau_c} \quad (5)$$

where $C(^1\text{H}) = (3/2) D^2 = (10/3) M_2^{\text{intra}}$, $C(^2\text{H}) = (3\pi^2/2) [\chi(^2\text{H})]^2$, and $C(^{17}\text{O}) = (12\pi^2/125) [\chi(^{17}\text{O})]^2$. For the data in Figure 3, we have used the ice *Ih* values for the intramolecular rigid-lattice second moment^{58,59} $M_2^{\text{intra}} = 19.6 \text{ G}^2$ and for the rigid-lattice quadrupole coupling constants⁶⁰⁻⁶² $\chi(^2\text{H}) = 213 \text{ kHz}$ and $\chi(^{17}\text{O}) = 6.5 \text{ MHz}$. These values should be appropriate for the approximately tetrahedrally hydrogen bonded internal water molecules of BPTI.^{10,27} The factor N_T in eq 5 removes the dependence on protein concentration, while the factor τ_c (and the use of $\omega_0\tau_c$ as abscissa) compensates for the small variation in the correlation time (*vide supra*).

Combination of eqs 1, 3, and 5 yields

$$R_1^{\text{scaled}} = N_T A^2 \left(\frac{0.2}{1 + (\omega_0\tau_c)^2} + \frac{0.8}{1 + (2\omega_0\tau_c)^2} \right) \quad (6)$$

The low-frequency limit of R_1^{scaled} in Figure 3 thus gives the quantity $N_T A^2$ directly. The precise scaling of the ^2H and ^{17}O data has been noted previously.¹³ The low-frequency value, $R_1^{\text{scaled}} = 2.04 \pm 0.04$, corresponds to the quite reasonable value $\langle A^2 \rangle = 0.68 \pm 0.01$ for the mean square generalized order parameter of the three internal water molecules W111, W112, and W113 in the G36S mutant. From the ^1H data, however, we obtain $R_1^{\text{scaled}} = 4.18 \pm 0.10$, corresponding to $\langle A^2 \rangle = 1.39 \pm 0.04$. This is an unphysical result since a dipolar order parameter cannot exceed 1. Although the A parameters for the different nuclei need not be equal (*vide infra*), the large deviation of the ^1H value indicates that the analysis is incomplete. In the following, we demonstrate that the large deviation of the scaled ^1H dispersion from the coincident ^2H and ^{17}O dispersions in Figure 3 is due to (i) a contribution from intermolecular dipole-dipole couplings between internal water and BPTI protons and (ii) a direct contribution from rapidly exchanging labile BPTI protons.

Figure 4 shows the WT - G36S difference dispersions for the three nuclei, scaled as in Figure 3. Since any direct labile proton contribution cancels out in the difference, all three dispersions must be due to the internal water molecule W122. In contrast to Figure 3, there is now a large difference between the scaled ^2H and ^{17}O dispersions as well. This difference is a consequence of the longer residence time of W122, $\tau_l = 170 \pm 20 \mu\text{s}$ at 27 °C,¹⁴ as compared to $\tau_l = 0.01 - 1 \mu\text{s}$ for W111 - W113.¹³ While W111 - W113 are in the fast exchange limit (with respect to the intrinsic relaxation rates of the internal water nuclei) for all three nuclei at 27 °C, W122 is in the fast exchange limit for ^1H only, in the intermediate exchange regime for ^2H , and nearly in the slow exchange limit for ^{17}O . This, in turn, is due to the different spin-lattice coupling constants for the three nuclei, causing the C factors (which are proportional to the intrinsic relaxation rates) in eq 5 to differ in the ratio 1:14.4:856 for ^1H , ^2H , and ^{17}O (assuming ice *Ih* coupling constants).

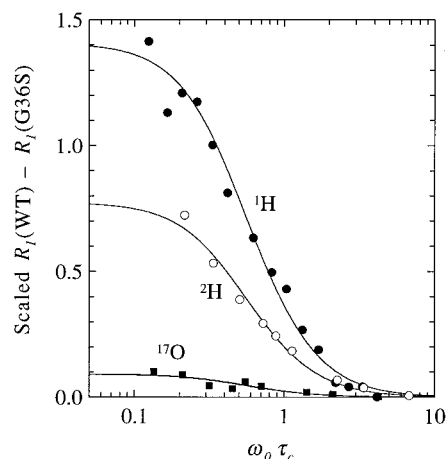


Figure 4. Water ^1H , ^2H , and ^{17}O difference dispersions (WT - G36S) at 27.0 °C. To allow a direct comparison, the data have been scaled as in eq 5. The curves resulted from two-parameter fits according to eq 1. The ^2H and ^{17}O data have been reported previously.¹³

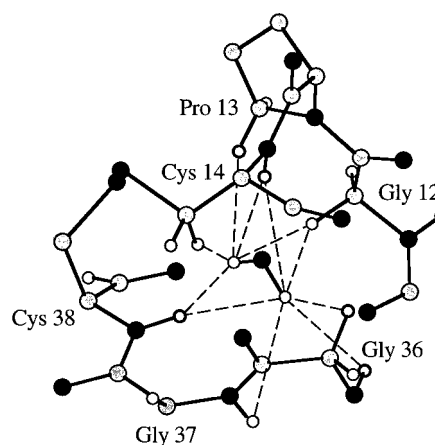


Figure 5. Environment of the internal water molecule W122 (center) in the crystal structure of BPTI.²⁷ The dashed lines represent the 11 intermolecular dipole couplings with H-H separations in the range 1.9–3.0 Å. Hydrogen atoms are white, carbon atoms grey, and N, O, or S atoms black. Negative NOEs have been observed with five (bold) of the eight strongly dipole-coupled BPTI protons.³⁹

A recent study of the temperature dependence (in the range 4–80 °C) of the ^2H and ^{17}O dispersions for WT and G36S BPTI indicates that W122 is fully ordered.¹⁴ We thus expect that $A_{\text{W122}}(^1\text{H}) = 1$. The low-frequency limit of $R_1^{\text{scaled}}(^1\text{H})$ in Figure 4, however, yields $A_{\text{W122}}^2(^1\text{H}) = 1.41 \pm 0.09$, implying that the effective dipole coupling constant is larger than the intramolecular ice value. This is indeed expected, since there are also intermolecular dipole couplings between the protons of W122 and nearby BPTI protons.

Intermolecular Dipole Couplings. In the crystal structure of BPTI,²⁷ the protons of the four internal water molecules are engaged in 40 intermolecular dipole couplings with proton separations less than 3 Å. This is illustrated in Figure 5 for the isolated internal water molecule W122. Such slowly modulated intermolecular dipole couplings give rise to characteristic positive cross-peaks in two-dimensional NOESY spectra^{39,40} and should also contribute substantially to the water ^1H relaxation dispersion.

When intermolecular as well as intramolecular dipole couplings are present, eq 1 should be replaced by

$$R_1(\omega_0) = R_{\text{bulk}} + \alpha + \beta_{\text{intra}} \tau_c F_{\text{intra}}(\omega_0\tau_c) + \beta_{\text{inter}} \tau_c F_{\text{inter}}(\omega_0\tau_c) \quad (7)$$

(58) Whalley, E. *Molec. Phys.* **1974**, *28*, 1105–1108.

(59) Rabideau, S. W.; Finch, E. D.; Denison, A. B. *J. Chem. Phys.* **1968**, *49*, 4660–4665.

(60) Edmonds, D. T.; Mackay, A. L. *J. Magn. Reson.* **1975**, *20*, 515–519.

(61) Spiess, H. W.; Garrett, B. B.; Sheline, R. K.; Rabideau, S. W. *J. Chem. Phys.* **1969**, *51*, 1201–1205.

(62) Edmonds, D. T.; Zussman, A. *Phys. Lett.* **1972**, *41A*, 167–169.

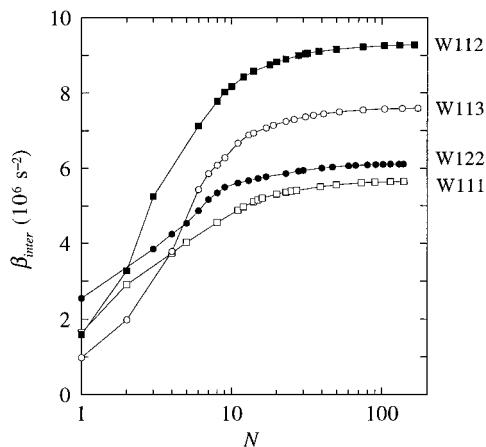


Figure 6. Dispersion amplitude parameter β_{inter} due to intermolecular dipole couplings with the indicated internal water molecules in BPTI. The data points were calculated as described in the text, using the crystal structure of BPTI. N is the number of BPTI protons within a prescribed radius R_{cut} of either of the two water protons. β_{inter} is inversely proportional to N_T ($= 3045$ here).

Table 2. Dispersion Amplitude Parameters β_{inter} and β_{cross} for Internal Water Molecules, Calculated from the Crystal Structure of BPTI with $R_{\text{cut}} = 10 \text{ \AA}$

water molecule	β_{inter} (10^6 s^{-2})	β_{cross} (10^6 s^{-2})
W111	5.65	-0.11
W112	9.28	-0.20
W113	7.60	-0.16
W122	6.12	-0.49
W111–W113	22.5	-0.46
all	28.7	-0.95

with the dispersion functions $F_{\text{intra}}(x) = 0.2/(1+x^2) + 0.8/(1+4x^2)$ and $F_{\text{inter}}(x) = 0.1 + 0.3/(1+x^2) + 0.6/(1+4x^2)$. The dispersion amplitude parameters in eq 7 are given by

$$\beta_{\text{intra}} = (1/N_T) \sum_{\mu}^3 \langle (D_{\mu}^{\text{intra}} A_{\mu}^{\text{intra}})^2 \rangle = (N_I/N_T) \langle (D^{\text{intra}} A^{\text{intra}})^2 \rangle \quad (8a)$$

$$\beta_{\text{inter}} = (1/N_T) \sum_{\mu} \sum_i \kappa_i \frac{1}{2} [(D_{\mu 1i}^{\text{inter}} A_{\mu 1i}^{\text{inter}})^2 + (D_{\mu 2i}^{\text{inter}} A_{\mu 2i}^{\text{inter}})^2] \quad (8b)$$

where D and A are the dipole coupling constant and order parameter associated with intramolecular and intermolecular dipole couplings (as indicated by a superscript). Further, the μ sum is over the N_I internal water molecules, the i sum is over all proton partners in long-lived intermolecular dipole couplings, and the subscripts 1 and 2 refer to the two protons in an internal water molecule. For intermolecular dipole couplings within the cluster of the three internal water molecules W111–W113, $\kappa_i = (3/2) F_{\text{intra}}(\omega_0\tau_c)/F_{\text{inter}}(\omega_0\tau_c)$ (“like spins”), while for dipole couplings to BPTI protons $\kappa_i = 1$ (“unlike spins”).

Using the hydrogen coordinates from the jointly refined neutron and X-ray crystal structure of BPTI,²⁷ we have calculated β_{inter} by including all N BPTI protons within a distance R_{cut} of either proton of a specified internal water molecule. For these calculations, the protein structure was taken to be rigid ($A_{\mu ni}^{\text{inter}} = 1$). The convergence of β_{inter} with increasing N is shown in Figure 6, and the converged values are collected in Table 2. A relatively large number of protons contribute significantly to β_{inter} , adding up to an intermolecular contribution of 1/3 of the experimental β (cf. Table 1).

Unfortunately, it is not possible to determine β_{intra} and β_{inter} separately by fitting eq 7 to the dispersion data. The reason is

that the frequency dependencies of the intra- and intermolecular contributions in eq 7, when properly normalized, are virtually indistinguishable. Thus, to *ca.* 1% accuracy, the dispersion functions $F_{\text{intra}}(x)$ and $F_{\text{inter}}(x)$ are related through $F_{\text{inter}}(x) = 0.1 + 0.9 F_{\text{intra}}(0.9x)$. If the minor shift of the dispersion frequency is neglected, eq 7 can therefore be cast on the form of eq 1, with the identifications

$$\alpha = \alpha_{\text{true}} + 0.1\beta_{\text{inter}}\tau_c \quad (9)$$

$$\beta = \beta_{\text{intra}} + 0.9\beta_{\text{inter}} \quad (10)$$

Since the fits in Figures 1 and 2 are based on eq 1, the parameter values in Table 1 should be interpreted according to eqs 9 and 10. The systematic error introduced by this approximate procedure was assessed by generating synthetic data with the aid of eq 7 and then comparing the quantities α , β , and τ_c obtained from a fit using eq 1 with the corresponding quantities calculated from eqs 9 and 10 using the input parameters. It was thus found that a fit based on eq 1 overestimates β by *ca.* 2% and underestimates τ_c by *ca.* 3%, while α is virtually unaffected by the approximation. These systematic errors are of little consequence for the present work and will henceforth be ignored.

With the data in Table 2, we find that the second term in eq 9 contributes merely 3–4% of the α value deduced from the WT and G36S dispersion fits in Figure 1. The foregoing interpretation of α is therefore hardly affected. As regards the difference dispersion in Figure 2, eq 9 predicts, with $\beta_{\text{inter}}(\text{W122})$ from Table 2, a high-field plateau value of 0.004 s^{-1} , rather than zero as assumed for the fit. This value, however, is just within the experimental uncertainty.

Intramolecular Dipole Coupling. Having estimated the intermolecular dipole couplings with the internal water molecules, we are now in a position to check whether the ^1H dispersion data are quantitatively consistent with the previously reported ^2H and ^{17}O dispersion data,^{13,14} *i.e.*, whether the intramolecular ^1H contribution corresponds to what is expected from four internal water molecules in wild-type BPTI and three in the G36S mutant.

The first step is to calculate β_{intra} from eq 10 with the values of β and β_{inter} taken from Tables 1 and 2, respectively. We use a rather conservative estimate of 20% for the uncertainty in the intermolecular contribution, corresponding roughly to an uncertainty of 0.1 \AA in the H–H distances in the protein structure. (From the high-resolution structures of three different crystal forms of BPTI,^{27,63,64} we calculate a root-mean-square variation of 0.05 \AA for the distances between the oxygen of W122 and eight heavy atoms within 4 \AA . This shows that the protein geometry, in this region at least, is not sensitive to environmental influences.) Including also the experimental error in β from the fit (cf. Table 1), we thus obtain $\beta_{\text{intra}} = (4.4 \pm 0.5) \times 10^7 \text{ s}^{-2}$ for G36S and $(1.5 \pm 0.2) \times 10^7 \text{ s}^{-2}$ for the WT – G36S difference dispersion.

The intramolecular dispersion amplitude parameter β_{intra} is related through eq 8a to the quantity $N_I \langle (D^{\text{intra}} A^{\text{intra}})^2 \rangle$. Since the difference dispersion is due exclusively to the internal water molecule W122, we have $N_I = 1$ here. Furthermore, from the ^2H and ^{17}O results,¹⁴ we have $A^{\text{intra}}(^1\text{H}) = 1$ (*vide supra*). If the G36S dispersion is ascribed to the three internal water molecules W111–W113, then $N_I = 3$. For both ^2H and ^{17}O , it was found that $N_I \langle A^2 \rangle = 2.04 \pm 0.04$.¹³ Since the electric field gradient tensors of these nuclei are of different geometry,^{12,52,60–62} the equality of the generalized order parameters implies a certain amount of orientational averaging by internal motions (on time scales shorter than protein tumbling). From its general defini-

tion, one can derive explicit expressions for A for each of the three librational normal modes. Such expressions have been presented for ^2H and ^{17}O .¹² For ^1H , a similar analysis shows that

$$[A^{\text{intra}}(^1\text{H})]^2 = 1 - 3\langle \sin^2 \phi \rangle \langle \cos^2 \phi \rangle \quad (11)$$

where ϕ is the angle of rotation around the libration axis. This result is valid for the twist and in-plane modes; the wag mode has no effect on A^{intra} . When the order parameters for the three nuclei are plotted versus the libration amplitude, it is found that under conditions where $A(^2\text{H})$ and $A(^{17}\text{O})$ converge to $(2.04/3)^{1/2}$, they also do not differ much from $A^{\text{intra}}(^1\text{H})$. We therefore adopt the value $N_I \langle (A^{\text{intra}})^2 \rangle = 2.04$ for the present analysis of the ^1H dispersion from the G36S mutant.

Using the values of β_{intra} and $N_I \langle (A^{\text{intra}})^2 \rangle$ deduced above, we can now use eq 8a to calculate the intramolecular dipole coupling constant D^{intra} . To facilitate comparison with other experimental data, however, we calculate instead the intramolecular second moment, $M_2^{\text{intra}} = (9/20) (D^{\text{intra}})^2$.⁵¹ We thus obtain $M_2^{\text{intra}} = 19 \pm 2 \text{ G}^2$ for W122 and $\langle M_2^{\text{intra}} \rangle = 28 \pm 3 \text{ G}^2$ as an average for W111–W113. We have previously argued^{10,11} that the strong and approximately tetrahedral hydrogen bonding of the internal water molecules in BPTI²⁷ implies that the water ^2H and ^{17}O quadrupole coupling constants should be essentially the same as in ice *Ih*. In the case of W122, where the most detailed data are available, this hypothesis appears to have been confirmed.¹⁴ If the present analysis of ^1H NMRD data is correct, we therefore expect the intramolecular second moment M_2^{intra} deduced for the internal water molecules in BPTI to closely match that of ice. Subtracting the calculated intermolecular second moment from the measured total second moment, one obtains $M_2^{\text{intra}} = 19.6 \pm 1.1 \text{ G}^2$ for ice *Ih*, $19.1 \pm 1.1 \text{ G}^2$ for ice *Ic*, $19.0 \pm 1.3 \text{ G}^2$ for ice *II*, and $20.3 \pm 1.3 \text{ G}^2$ for ice *IX*.^{58,59} Our result for W122 is thus in excellent agreement with the ice values, as anticipated. For W111–W113, however, the deduced average intramolecular second moment of $28 \pm 3 \text{ G}^2$ is significantly larger than in any of the ice polymorphs. This finding indicates a non-negligible contribution to the water ^1H relaxation from labile BPTI protons at pH 5.1.

It should be noted that the quoted intramolecular second moments for the ice polymorphs include the effect of motional averaging by intramolecular vibrations and small-amplitude librations.^{65,66} While these motions have been estimated to reduce M_2^{intra} by 16%,⁵⁸ they are much too fast (10–100 fs) to make a significant direct contribution to the relaxation. (Motional averaging by slower motions, typically a few to a few hundred picoseconds, is taken into account *via* the order parameter A .) The high-frequency motional averaging should occur to roughly the same extent for water molecules in ice and in proteins. Also the ice values for the ^2H and ^{17}O quadrupole coupling constants are motionally averaged in this way.

Exchange of Labile BPTI Protons. The water ^1H and ^2H relaxation rates from a protein solution generally include direct contributions from labile protein hydrogens exchanging with water.^{11,57} In the case of BPTI, the strong observed pD dependence of the ^2H dispersion amplitude parameter β can be quantitatively accounted for by exchanging labile hydrogens.¹¹ Only in a narrow range around pD 5.5 can this effect be

neglected. Due to the smaller coupling constant for ^1H , the intrinsic relaxation time of a labile proton is 1–2 orders of magnitude longer than for the corresponding labile deuteron. Consequently, labile hydrogen exchange is expected to be more important for the ^1H dispersion.

To incorporate the effect of exchanging labile protons on the ^1H relaxation, we decompose the dispersion amplitude into contributions from internal water molecules (β_W) and from labile protons in the protein (β_P)

$$\beta = \beta_W + \beta_P \quad (12)$$

where $\beta_W = \beta_{W,\text{intra}} + 0.9\beta_{W,\text{inter}}$ as in eq 10, with $\beta_{W,\text{intra}}$ and $\beta_{W,\text{inter}}$ given by eqs 8a and 8b. Also the β_P term has “intramolecular” (within NH_2 and NH_3 groups) and “intermolecular” parts. If proton exchange is fast compared to the intrinsic relaxation, β_P is simply related to a population-weighted average of intrinsic relaxation rates. At a given pH, however, the labile proton population exhibits a wide range of exchange rates. We therefore compute β_P as

$$\beta_P = [R_P(0) - R_P(\omega_\alpha)]/\tau_c \quad (13)$$

where ω_α is a frequency on the α plateau above the β dispersion, and

$$R_P(\omega) = \frac{1}{2(N_T + N_P)} \sum_k \frac{N_{Pk}}{T_{Pk}(\omega) + \tau_{Pk}} \quad (14)$$

where the sum runs over all labile groups in the protein. N_{Pk} is the number of protons in each group, determined by solution pH and $\text{p}K_a$ values for the labile protons, all of which are known for BPTI.⁶⁷ Furthermore, $N_P = \sum_k N_{Pk}$. The mean residence times τ_{Pk} of labile protons are determined by pH and the rate constants for acid- and base-catalyzed proton exchange, many of which have been determined for BPTI.^{11,28,29} For the present calculations, we made use of the known rate constants, corrected to 27 °C using estimated activation energies.^{28,68} For those labile protons where rate constants have not been determined, we used values for similar labile protons in BPTI or in model compounds.⁶⁸ Finally, to achieve agreement with the isotope dilution data (*vide infra*), we scaled the hydroxyl rate constants by a factor 3 and the lysine rate constant by a factor 0.3 (giving $k_2 = 6.5 \times 10^9 \text{ M}^{-1} \text{ s}^{-1}$, in close agreement with a previous estimate for BPTI¹¹). The intrinsic relaxation times $T_{Pk}(\omega)$ of labile protons were calculated from the proton coordinates in the crystal structure of BPTI.²⁷ In this way we obtained $\beta_P = 1.5 \times 10^7 \text{ s}^{-2}$ at 27 °C, pH 5.1 and $N_T = 3045$. For the following analysis, we estimate the uncertainty in β_P to 20%.

The intramolecular contribution from the three internal water molecules W111–W113 can now be obtained as $\beta_{W,\text{intra}} = \beta - 0.9\beta_{W,\text{inter}} - \beta_P = (2.9 \pm 0.5) \times 10^7 \text{ s}^{-2}$. Inserting this value and $N_I \langle (A^{\text{intra}})^2 \rangle = 2.04$ (*vide supra*) into eq 8a, we arrive at the (average) intramolecular second moment $\langle M_2^{\text{intra}} \rangle = 18 \pm 4 \text{ G}^2$ for W111–W113. The close agreement of this value with M_2^{intra} for the ice polymorphs (*vide supra*) supports our independent estimate of β_P .

The WT – G36S difference dispersion should be unaffected by proton exchange since the β_P contribution cancels out in the difference. The G36S mutant contains, in addition, the hydroxyl group of Ser 36. Being deeply buried and strongly hydrogen bonded, however, this hydroxyl proton should exchange too slowly to contribute significantly even to the ^1H dispersion.²⁰

(63) Wlodawer, A.; Deisenhofer, J.; Huber, R. *J. Mol. Biol.* **1987**, *193*, 145–156.

(64) Wlodawer, A.; Nachman, J.; Gilliland, G. L.; Gallagher, W.; Woodward, C. *J. Mol. Biol.* **1987**, *198*, 469–480.

(65) Pedersen, B. *J. Chem. Phys.* **1964**, *41*, 122–132.

(66) Barmaal, D. E.; Lowe, I. J. *J. Chem. Phys.* **1967**, *46*, 4800–4809.

(67) Wüthrich, K.; Wagner, G. *J. Mol. Biol.* **1979**, *130*, 1–18.

(68) Liepinsh, E.; Otting, G. *Magn. Reson. Med.* **1996**, *35*, 30–42.

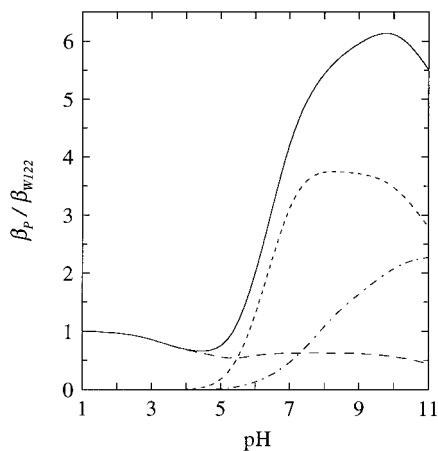


Figure 7. Variation with pH of the labile proton contribution β_P to the ^1H dispersion from BPTI solutions at 27 °C, calculated as described in the text. β_P has been normalized by the contribution β_{W122} of one fully ordered internal water molecule (W122); the ratio is thus independent of protein concentration. Separate contributions to β_P are shown from the OH and COOH groups (long dash), the lysines and arginines (short dash), and the amides (dash-dot) of BPTI.

At pH 5.1 and 27 °C, the β_P contribution is dominated by the eight hydroxyl protons in BPTI (*ca.* 70%), which are in the fast exchange limit with τ_{Pk} in the range 0.5–5 ms and $T_{Pk}(0)$ in the range 8–40 ms. The 15 ammonium protons in BPTI, which also contribute significantly (*ca.* 15%) to β_P , have intermediate exchange rates at pH 5.1 ($\tau_{Pk} \approx T_{Pk}$ in the range 20–85 ms). At higher pH values, arginine and amide protons make large contributions to β_P , and at lower pH there is a small contribution from rapidly exchanging carboxylic protons. Figure 7 shows the variation of β_P with pH at 27 °C, calculated as described above. In calculating the curves in Figure 7, order parameters of 0.6 were used for the flexible side chains of lysine and arginine residues,¹¹ where relaxation is predominantly intramolecular. (In addition, we assumed fast rotation of NH_3 groups.) For other types of labile protons, relaxation is intermolecular and therefore less affected by internal motions. In Figure 7, the labile proton contribution, β_P , has been normalized by the contribution, $\beta_W = 2.0 \times 10^7 \text{ s}^{-2}$, from a fully ordered internal water molecule such as W122. Above pH 6.4, the labile proton contribution to the ^1H dispersion amplitude exceeds that from the four internal water molecules. The long-standing belief that labile proton contributions are negligible at neutral pH^{8,16–18,22,30,31} is clearly not supported by the present analysis. On the other hand, the results of Figure 7 show the expected qualitative similarity with the previously reported pH dependence of the ^2H dispersion amplitude.¹¹

Isotope Dilution. By recording the ^1H relaxation dispersion from protein solutions of varying H/D isotope composition, the contribution from intermolecular dipole couplings with nonlabile protein protons can be isolated.^{4,21–26} Figure 8 shows the result of such an isotope dilution experiment on four BPTI solutions of varying atom fraction deuterium (x) in the exchanging hydrogen pool (water and labile hydrogens). The dispersion parameters α , β , and τ_c in eq 1, resulting from the fits shown in Figure 8, are collected in Table 3. All four solutions were of the same BPTI concentration, slightly higher (18.9 mM, or $N_T = 2600$) than in the solutions used for the difference NMRD experiment (16.8 mM or $N_T = 3045$). The lyonium ion activity was also the same in the four solutions, with pL = pH* + 0.4x = 5.1, as in the difference NMRD experiment. As expected, the β values in Table 1 (wild-type BPTI) and Table 3 ($x = 0$) coincide when normalized by the concentration variable N_T .

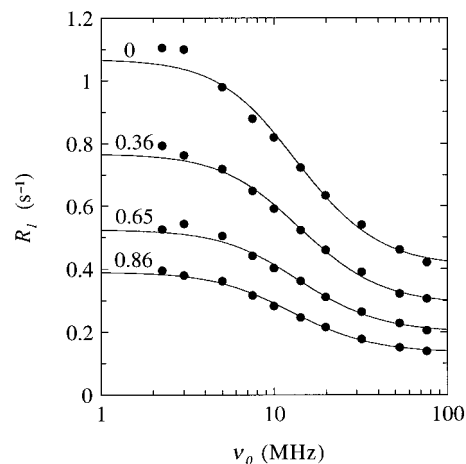


Figure 8. Dispersion of the water ^1H longitudinal relaxation rate in 18.9 mM BPTI solutions with isotopically mixed water (deuterium fraction indicated) at 27.0 °C and pL 5.1. The curves resulted from three-parameter fits according to eq 1. Except for the two lowest frequencies, the estimated error bars (*ca.* 1%) are roughly the same size as the data symbols.

Table 3. Parameter Values Deduced from Fits of Eq 1 to the ^1H Relaxation Dispersion Data in Figure 8

x	$R_{\text{bulk}} + \alpha \text{ (s}^{-1}\text{)}$	$\beta \text{ (} 10^7 \text{ s}^{-2}\text{)}$	$\tau_c \text{ (ns)}$
0	0.409 ± 0.004	10.0 ± 0.2	6.6 ± 0.2
0.360	0.289 ± 0.003	7.48 ± 0.16	6.4 ± 0.2
0.651	0.199 ± 0.002	5.08 ± 0.11	6.4 ± 0.2
0.856	0.134 ± 0.001	3.61 ± 0.07	7.1 ± 0.2

Due to the smaller magnetic moment of the deuteron, a uniform H \rightarrow D substitution reduces the ^1H relaxation rate by a factor $^{2/3}(\gamma_D/\gamma_H)^2 I_D(I_D + 1)/I_H(I_H + 1) = 0.042$.^{51,69} If the H_2O solvent in a protein solution is replaced by D_2O , all contributions to the dispersion amplitude β from (intra- and intermolecular) dipole couplings with labile hydrogens (including internal water hydrogens) are therefore reduced by this factor, while contributions from (intermolecular) dipole couplings with nonlabile protein protons are unaffected. In an isotopically mixed solvent ($0 < x < 1$), a proton dipole-coupled to n hydrogen nuclei can exist in 2^n states with different H/D substitution patterns and, hence, different intrinsic relaxation rates. If H/D exchange is fast compared to spin relaxation, however, the intrinsic relaxation rates will be population-weighted averages over the ensemble of H/D configurations. Consequently, the dispersion amplitude should decrease linearly with the deuterium fraction as

$$\beta(x) = \beta_0 + (1 - 0.958x)\beta_1 \quad (15)$$

where β_0 and β_1 are the contributions from dipole couplings with nonlabile and labile protons, respectively.

Figure 9 shows the variation of β with x for BPTI at pL 5.1. Within the experimental uncertainty, the linear relationship in eq 15 is obeyed. (In the fast exchange regime, β is unaffected by the isotope effect on solvent viscosity.) The solid curve, which conforms closely to the data, was calculated as follows. The water contribution β_W (dashed line) was obtained from the $\beta_{W,\text{intra}}$ and $\beta_{W,\text{inter}}$ values deduced from the preceding analysis (and scaled to $N_T = 2600$), with $\beta_{W,\text{inter}}$ partitioned into β_0 and β_1 contributions on the basis of the crystal structure. For W122, 57% of $\beta_{W,\text{inter}}$ is due to dipole couplings with labile protons, essentially the amide NH protons of Cys 14, Gly 36, and Cys 38 (*cf.* Figure 5). The percentage is nearly the same for the

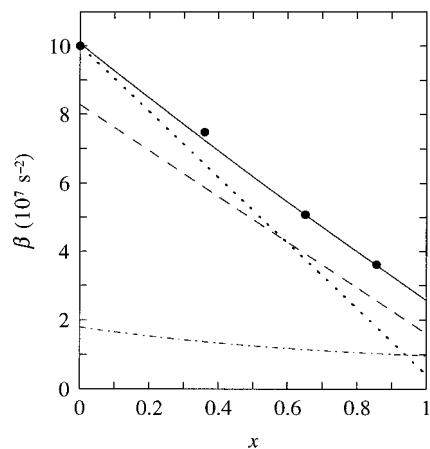


Figure 9. Variation of the dispersion amplitude parameter β with the D atom fraction x . The solid curve, calculated as described in the text, is the sum of a contribution β_w from the four internal water molecules (dashed line) and a contribution β_p from labile BPTI protons (dash-dotted curve). The expected reduction of β with x in the absence of dipole couplings to nonlabile BPTI protons is also shown (dotted line).

four internal water molecules as a group. The contribution β_p from exchanging BPTI protons (dash-dotted curve) was calculated from eqs 13 and 14, using the same rate constants as for the preceding analysis. The nonlinearity in this contribution is due to the lysine NH_3 protons that are in the intermediate exchange regime (*cf.* eq 14). In principle, a nonlinear x dependence can also result from the (primary) isotope effects on $\text{p}K_a$ values and $\text{p}K_w$ (included in the analysis), from the (secondary) isotope effects on the exchange rate constants (neglected), and from small deviations of isotope fractionation factors⁷⁰ from unity (neglected). At least under the present conditions, however, these effects are insignificant.

As a convenient indicator of the relative importance of dipole couplings with labile and nonlabile protons, we take the relative reduction of β on going from H_2O to D_2O . This quantity, denoted $\Delta\beta$, is proportional to the slope of a linear $\beta(x)$ plot. For BPTI at pH 5.1, we find $\Delta\beta = 75\%$, clearly less than the 96% expected if all dipole couplings involved labile protons (dotted line in Figure 9). The nonlabile BPTI protons responsible for this difference are dipole-coupled to internal water molecules (β_w) as well as to exchanging BPTI protons (β_p). The β_w contribution, with $\Delta\beta_w = 81\%$, is dominated by the intramolecular dipole coupling. The β_p contribution at pH 5.1 is dominated by the eight hydroxyl protons ($\Delta\beta_{\text{OH}} = 31\%$). The 15 ammonium protons add a smaller nonlinear (intermediate exchange rate) contribution with a larger reduction factor (due to the dominant intramolecular dipole couplings within the NH_3 group).

In several earlier ^1H NMRD studies of protein solutions, the behavior of the water ^1H relaxation rate under H/D isotope dilution has been taken as evidence for significant cross-relaxation between the labile and nonlabile proton pools.^{3,22,24,26} The present analysis shows, however, that the isotope dilution data can be quantitatively accounted for without invoking cross-relaxation. This conclusion is supported by the theoretical analysis of cross-relaxation described in the following section.

We shall not attempt to analyze the x dependence of α (Table 3). To do this, the dispersion should be extended to higher frequencies to define the high-frequency plateau more accurately. Fortunately, the uncertainty in the present data in this respect are of little consequence for the analysis of β (since $\beta\tau_c$ is large compared to α).

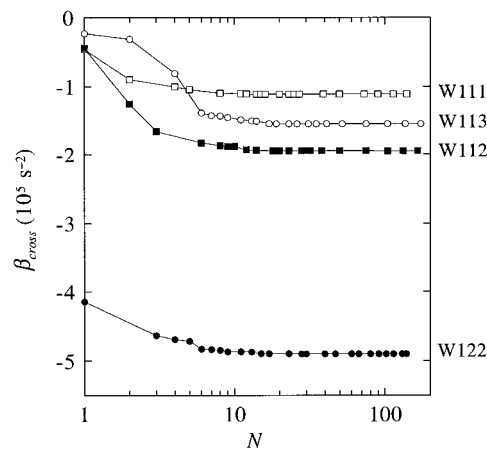


Figure 10. Dispersion amplitude parameter β_{cross} due to cross-relaxation between BPTI protons and the protons of the indicated internal water molecules. The data points were calculated as described in the text, using the crystal structure of BPTI. N is the number of BPTI protons within a prescribed radius R_{cut} of either of the two water protons. β_{cross} is inversely proportional to N_T ($= 3045$ here).

Dipolar Cross-Relaxation. In the preceding analysis, we assumed that intramolecular and intermolecular dipole couplings contribute additively to R_1 as in eq 7. This is an approximation. A more rigorous approach is to calculate the evolution of the observed water magnetization for the case where a water molecule (or labile proton) exchanges between the bulk solvent and an internal site, where each of the water protons is dipole coupled to the protein protons, which in turn are dipole coupled to each other.

In the Appendix, we present a rigorous treatment of dipole relaxation in a multispin system in the presence of chemical exchange. This analysis shows that eq 7 should be supplemented by a term of the form $\beta_{\text{cross}}\tau_c F_{\text{cross}}(\omega_0\tau_c)$, where, like $F_{\text{intra}}(x)$ and $F_{\text{inter}}(x)$, $F_{\text{cross}}(x)$ is a non-negative dispersion function with normalization $F_{\text{cross}}(0) = 1$. The cross-relaxation term cannot in general be expressed in a simple form but can be evaluated numerically as described in the Appendix. As for β_{inter} , we have calculated β_{cross} for the four internal water molecules in BPTI, using the proton coordinates in the crystal structure²⁷ and including N BPTI protons within a distance R_{cut} of either water proton. The results are presented in Figure 10 and Table 2. The cross-relaxation term β_{cross} is very small, about 1% of β , and, as anticipated (*cf.* Appendix), it is negative. In the investigated frequency range, the dispersion function is well approximated by $F_{\text{cross}}(x) = [1.2/(1 + 4x^2) - 0.2]^2/F_{\text{inter}}(x)$, which is the exact result for $N = 1$ (*cf.* eq A14). With a correlation time of $\tau_c = 6.2$ ns, as found here, the cross-relaxation contribution should thus produce a broad maximum just below 30 MHz. Since β_{cross} is expected to be merely 1% of β , however, this feature cannot be resolved at the present experimental accuracy (*ca.* 1% in R_1). Similar calculations were performed for the labile protons of BPTI, yielding (negative) cross-relaxation corrections to the intrinsic relaxation rates of at most a few percent.

While the present numerical assessment of cross-relaxation effects refers specifically to BPTI, the spatial distribution of protons around the four internal water molecules and elsewhere in the protein structure should be fairly typical of globular proteins in general. The conclusion that cross-relaxation is unimportant for the ^1H relaxation should therefore hold generally for solutions of freely tumbling proteins. The relative importance of cross-relaxation is determined by quantities of the form $\sigma_{ij}^2/(\rho_i\rho_j)$. Since the cross-relaxation rate σ_{ij} is due solely to the dipole coupling between protons i and j , while the auto-

(70) Schowen, K. B.; Schowen, R. L. *Meth. Enzymol.* **1982**, *87*, 551–606.

relaxation rates ρ_i and ρ_j involve all dipole couplings to these protons (cf. eq A3), one expects in general that $\sigma_{ij}^2 \ll \rho_i\rho_j$. This is particularly obvious when i or j is a water proton, strongly coupled to its intramolecular partner. Since this argument is independent of the value of the correlation time τ_c , cross-relaxation should be unimportant also for proteins that are much larger than BPTI or dissolved in highly viscous solvents, as long as the conventional perturbation theory of spin relaxation is valid.

Due to the pseudoadiabatic spectral density, $j(\omega_i - \omega_j) \approx j(0)$, present in σ_{ij} and ρ_{ij} , cross-relaxation has a small but significant effect on the α plateau, above the β dispersion. In the case of W122, which shows the largest cross-relaxation effect among the four internal water molecules in BPTI (cf. Table 2), the high-frequency intermolecular contribution to R_1 , as given by the second term in eq 9, is thus reduced by ca. 50% due to cross-relaxation. Since the high-frequency intermolecular contribution is merely a few percent of the surface water contribution α , however, cross-relaxation can be ignored also at high frequencies. A longer correlation time τ_c , whether due to a larger protein or a more viscous solvent, would not alter this conclusion much, since both terms in eq 9 would increase. For the magnetization associated with the nonlabile protein protons (not observed here), however, cross-relaxation can become important at high frequencies for large proteins.^{71,72}

Conclusions

Over the past three decades, numerous attempts have been made to define the respective roles of hydration water, labile protons, intra- and intermolecular dipole couplings, and cross-relaxation in determining the water ^1H relaxation rate measured in protein solutions.^{5–8} The failure of this massive body of experimental data to provide a coherent picture of protein–water interactions and dynamics was due mainly to the incomplete understanding of the molecular mechanism whereby hydration water acquires a correlation time 3–4 orders of magnitude longer than in bulk water. The recent demonstration^{9–15} by ^{17}O NMRD of the crucial role played by internal water molecules also removed the major obstacle to a molecular interpretation of ^1H relaxation data from protein solutions.

Taken together with the previous ^2H and ^{17}O NMRD studies of wild-type and mutant BPTI,^{9–11,13,14} the present ^1H NMRD study of the same proteins demonstrates that the relaxation dispersions of all three nuclei report on internal water molecules exchanging with bulk water on a time scale that is short compared to the intrinsic relaxation time. For all three nuclei, the coupling constant for the internal water molecules is consistent with that in hexagonal ice, as expected from the similar hydrogen bond geometry.

The relaxation rates of the hydrogen isotopes contain, in addition, a direct contribution from exchanging protein hydrogens which generally is more important for ^1H than for ^2H , due to the longer intrinsic relaxation time of ^1H . While the ^2H dispersion may be virtually unaffected by hydrogen exchange in a narrow pH range, as found for BPTI,¹¹ the ^1H dispersion appears to be affected under all conditions. For BPTI at neutral pH, labile protein protons thus make a larger contribution than water protons to the ^1H relaxation dispersion. For its relatively small size (6.5 kDa), BPTI has an unusually high internal water content. The labile proton contribution is therefore expected to be relatively more important for most other proteins. It is

clear that pH is a crucial variable in water ^1H relaxation studies of aqueous macromolecular systems. Conclusions drawn from previous ^1H studies where the labile proton contribution was ignored (sometimes to the extent that pH was not even reported) need to be reexamined. Moreover, the present results suggest that labile protons play an important, if not dominant, role in determining magnetization transfer contrast in magnetic resonance imaging of soft tissue.

As demonstrated previously for $^2\text{H}^{13,14}$ and here for ^1H , the labile hydrogen contribution may be eliminated by performing a difference NMRD experiment involving mutants or otherwise modified proteins. Under such conditions, the ^1H dispersion can usefully complement ^2H and ^{17}O data in several respects. First, due to the widely different coupling constants and consequent difference in intrinsic relaxation times, the three nuclei have different “NMRD windows”,^{14,15} i.e., they are sensitive to internal water molecules with residence times in different ranges. By comparing the dispersions of the three nuclei, more detailed information about residence times can thus be obtained. Second, due to the different geometries of the interaction tensors of the three nuclei, they are affected to a different extent by anisotropic motions of internal water molecules. A fast 180° flip around the water dipole axis, for example, reduces the ^2H dispersion amplitude by 40% but has no effect on the ^1H and ^{17}O amplitudes.¹² Third, due to the much higher magnetogyric ratio of ^1H as compared to ^2H and ^{17}O , the ^1H dispersion can be followed up to much higher frequencies, approaching the GHz range. This is an advantage in studies of small proteins, high temperatures, or short residence times.

In previous work, the role of intermolecular dipole couplings and cross-relaxation has been assessed by comparing ^1H and ^2H NMRD profiles from protein solutions.^{5,16,22,30} For all investigated proteins, the scaled ^1H rate is found to be considerably larger than the scaled ^2H rate. In the past, the scaling has usually been done with the bulk water relaxation rates. Since the intermolecular contribution to the ^1H rate is ca. 60% in bulk water,⁷³ as compared to ca. 30% for an isolated internal water molecule such as W122 (cf. Tables 1 and 2), scaling with bulk water rates tends to underestimate the intermolecular contribution (producing a too low scaled $^1\text{H}/^2\text{H}$ ratio) and may obscure a direct labile proton contribution. Given that the water contribution (β_w) is due to internal water molecules, it is more natural to scale the relaxation rates with the rigid-lattice (ice *Ih*) coupling constants, as in eq 5. The ratio of the scaled dispersion amplitudes is then given by the quantity $K = [\beta(^1\text{H})/\beta(^2\text{H})][C(^2\text{H})/C(^1\text{H})]$. The data in Figures 3 and 4 yield $K = 1.8$ for W122 and $K = 2.1$ for W111–W113 in BPTI solutions at pH 5.1 and 27 °C. From previously reported data, we obtain $K = 2.6$ for carbonmonoxy hemoglobin (pH 7.5, 25 °C),³⁰ $K = 3.5$ for lysozyme (pH 4.5, 22 °C),³⁰ and $K = 6.8$ for alkaline phosphatase (pH 7.5, 5 °C).²² As shown here, a value $K > 1$ can be attributed to any or all of the following effects: (i) an intermolecular ^1H auto-relaxation contribution, (ii) a direct labile hydrogen contribution, which is always larger for ^1H than for ^2H , (iii) internal water molecules that are not in the fast exchange limit and therefore contribute more to ^1H than to ^2H (cf. Figure 4), and (iv) internal water molecules that undergo fast 180° flips, which only reduce the ^2H rate. In the absence of effects (ii)–(iv), we expect $K \approx 1.3$ for singly buried water molecules (as W122) and $K \approx 1.6$ for linear clusters of buried water molecules (as W111–W113). The considerably larger K values actually obtained indicate that

(71) Kalk, A.; Berendsen, H. J. C. *J. Magn. Reson.* **1976**, *24*, 343–366.

(72) Sykes, B. D.; Hull, W. E.; Snyder, G. H. *Biophys. J.* **1978**, *21*, 137–146.

(73) Lankhorst, D.; Schriever, J.; Leyte, J. C. *Ber. Bunsenges. Phys. Chem.* **1982**, *86*, 215–221.

the effects (ii)–(iv) are important. For the proteins studied at pH 7.5, the direct labile proton contribution probably exceeds the water contribution (*cf.* Figure 7).

Previous H/D isotope dilution studies have not produced a coherent picture of the role of intermolecular dipole couplings. Three factors are mainly responsible for this: (i) the importance of internal water molecules was not recognized, (ii) the direct labile proton contribution was usually ignored, and (iii) paramagnetic impurities may have contributed to the ^1H rate at high deuterium fractions.^{21,30} By explicitly calculating the contribution from exchanging and nonexchanging protein protons to the intermolecular dipole couplings with internal water molecules and labile protons, we have shown here that the measured β reduction, $\Delta\beta = 75\%$, for BPTI at pH 5.1 can be quantitatively accounted for. Previously reported ^1H NMRD isotope dilution data yield smaller β reductions than found here: $\Delta\beta = 59\%$ for fibrinogen (pH 5.9 and 7.3, 28 °C),²⁵ $\Delta\beta = 59\%$ for carbonic anhydrase (pH 7.5, 5 °C),²² $\Delta\beta = 48\%$ for carbonmonoxy hemoglobin (pH 7.5, 25 °C),²² and $\Delta\beta = 31\%$ for alkaline phosphatase (pH 7.5, 5 °C).²² The smallest $\Delta\beta$ is expected from labile OH and NH protons, which relax entirely by intermolecular dipole couplings. Among the proteins mentioned, alkaline phosphatase has a uniquely high (OH + NH)/(NH₂ + NH₃) ratio, which may partly explain the small $\Delta\beta$ value.

In one previous isotope dilution study,²² the reported plots of $\beta\tau_c$ versus x were concave upwards at high x . This finding cannot be explained by the small nonlinear isotope effects on β discussed here. In fact, one would expect the curvature to be concave downwards due to the viscosity isotope effect on τ_c . Since the reported dispersion amplitudes were determined by fitting the empirical Cole–Cole dispersion to dispersion data that do not extend up to the α plateau, it is possible that systematic errors play a role. Such errors are expected to be most important at high x , where the dispersion is small. Nonlinearities are absent in the present BPTI data (extending up to $x = 0.86$) as well as in previously reported data for fibrinogen²⁵ and lysozyme²⁶ (both these studies extended up to $x = 0.90$). Other isotope dilution studies^{4,21,23} have been restricted to a single relatively high resonance frequency and therefore report mainly on the α contribution from surface hydration.

Earlier theoretical treatments of the effect on water ^1H relaxation of cross-relaxation with protein protons have generally been based on phenomenological models, postulating two or more proton “phases”, each with a uniform “spin temperature” established by “spin diffusion”, taken to be fast compared to longitudinal relaxation.^{5,22,41–43} These concepts are borrowed from the solid state, where the flip-flop term in a static dipolar Hamiltonian leads to coherent polarization transfer, often referred to as spin diffusion.⁷⁴ For a protein solution, where the dipolar Hamiltonian fluctuates at a rate fast compared to the dipole couplings (the motional narrowing condition), these concepts are no longer applicable. In particular, the cross-relaxation rates σ_{WP} are typically much smaller than the auto-relaxation rates ρ_W and ρ_P , thus effectively quenching polarization transfer. Within the framework of the phenomenological model, cross-relaxation is regarded as a consequence of a higher intrinsic longitudinal relaxation rate of protein protons as compared to water protons, the former acting as a relaxation sink for the latter. The appearance in this model of a cross-relaxation rate constant with a physical significance that is qualitatively different from the cross-relaxation rate in the Solomon equations^{32,33} has created considerable confusion. Now that the origin of the relaxation dispersion has been identified

as internal water molecules and labile protons, it is straightforward to calculate the cross-relaxation contribution using the rigorous Solomon equations. When this is done, it is found that the cross-relaxation effect on the ^1H relaxation dispersion is negligible. It is also clear that the high-frequency α contribution is virtually unaffected by cross-relaxation. This conclusion follows since the quantity $\sigma_{WP}^2/(\rho_W\rho_P)$, which determines the efficiency of cross-relaxation (*cf.* Appendix), is proportional to the effective correlation for the ρ_W and ρ_P rates, and this cannot exceed the subnanosecond residence time of a water molecule at the protein surface.

The suggestion by Edzes and Samulski^{41,75} that cross-relaxation plays a role for water ^1H relaxation in macromolecular systems was based on experimental data from biological systems that differ in two important respects from protein solutions: the macromolecules were not free to tumble, and the water content was low. Under these conditions, the theoretical treatment presented here does not apply, and a significant role for cross-relaxation cannot be ruled out. Ironically, the current view of the leading proponent for cross-relaxation effects in mobile protein solutions is that cross-relaxation is unimportant for cross-linked proteins.^{19,76} Instead, the distinctly non-Lorentzian ^1H dispersion from cross-linked serum albumin was interpreted in terms of two classes of long-lived water molecules at the protein surface, with residence times of 1 μs and 23 ns, respectively.^{19,76} A similar interpretation was proposed for the ^2H dispersion in the same system.¹⁸ As we have demonstrated elsewhere,^{77,78} however, the ^2H dispersion frequency in a rotationally immobilized system reflects the (residual) quadrupole frequency rather than a motional correlation time. Analogous considerations should apply to the ^1H dispersion.

In their recent work, Koenig and co-workers attempt to redefine the concept of cross-relaxation.^{76,79} The pseudo-adiabatic spectral density $j(0)$, appearing in the auto- and cross-relaxation rates (*cf.* eqs A4 and A5), is thus said to be associated with “magnetization transfer”, the spectral density $j(\omega_0)$ with “cross-relaxation”, and the spectral density $j(2\omega_0)$ with both. In our view, this semantic exercise does little to clarify the issue. We use the term cross-relaxation in its original sense^{32,33} to describe the dynamic coupling between the longitudinal magnetizations of different spin populations. The theoretical analysis presented here shows that the effect of this coupling on the water ^1H relaxation dispersion in protein solutions is negligible. The intrinsic ^1H relaxation rates of internal water molecules and labile protein protons can therefore be obtained by simply adding the intermolecular auto-relaxation rate to any intramolecular contribution, as in eq 7. Since, in protein solutions, the water ^1H relaxation rate should be virtually unaffected by the relaxation (or saturation) of the magnetization associated with the nonexchanging protein protons, there is no need to consider coupled equations of motion.

Acknowledgment. We are grateful to Drs. Hörlein and Peters of Bayer AG, Wuppertal, Germany for a generous gift of the BPTI G36S mutant, and to Novo Nordisk A/S, Gentofte, Denmark for a generous gift of recombinant BPTI. This work was supported by the Swedish Natural Science Research Council (NFR).

(75) Edzes, H. T.; Samulski, E. T. *Nature* **1977**, *265*, 521–523.

(76) Koenig, S. H.; Brown, R. D. *Magn. Reson. Med.* **1993**, *30*, 685–695.

(77) Halle, B.; Denisov, V. P. *Biophys. J.* **1995**, *69*, 242–249.

(78) Halle, B. *Progr. NMR Spectrosc.* **1996**, *28*, 137–159.

(79) Koenig, S. H. In *Encyclopedia of Nuclear Magnetic Resonance*; Grant, D. M., Harris, R. K., Eds.; Wiley: New York, 1995; pp 4108–4120.

(74) Meier, B. H. *Adv. Magn. Opt. Reson.* **1994**, *18*, 1–116.

Appendix: Dipole Relaxation in a Multispin System with Chemical Exchange

Consider a spin-1/2 nucleus exchanging between a bulk-like environment and a macromolecular site, where it is dipole coupled to N macromolecular spin-1/2 nuclei, all of which are mutually dipole coupled. The exchanging nucleus might be a proton in a water molecule exchanging between a bulk environment and an internal cavity in a protein or a labile protein proton exchanging with bulk water. We assume that all spins are weakly coupled, *i.e.*, all scalar J couplings are small compared to the corresponding chemical shift differences. Furthermore, we assume that all spins have the same magnetogyric ratio, γ . Finally, we neglect cross-correlations, *i.e.*, we consider only auto-correlation functions for the spatial variables.

Under the stipulated conditions, the coupled evolution of the nonequilibrium longitudinal magnetization associated with the considered spins is described by a set of $N + 2$ linear relaxation-exchange equations,^{32,33} that can be expressed in matrix notation as

$$\frac{d}{dt}\mathbf{X}(t) = -\mathbf{R}\mathbf{X}(t) \quad (\text{A1})$$

where $\mathbf{X}(t)$ is a column vector with components $[\Delta I_{zB}, \Delta I_{zM}, \Delta I_{z1}, \Delta I_{z2}, \dots, \Delta I_{zN}]$, the subscripts labeling the bulk-like state (B), the exchanging macromolecular site (M), and the non-exchanging macromolecular sites (1,2,...,N). The rate matrix \mathbf{R} takes the form

$$\mathbf{R} = \begin{bmatrix} (\rho_B + fk) & -k & 0 & 0 & \cdots & 0 \\ -fk & (\rho_M + k) & \sigma_{M1} & \sigma_{M2} & \cdots & \sigma_{MN} \\ 0 & \sigma_{M1} & \rho_1 & \sigma_{12} & \cdots & \sigma_{1N} \\ 0 & \sigma_{M2} & \sigma_{12} & \rho_2 & \cdots & \sigma_{1N} \\ \vdots & \vdots & \vdots & \vdots & \ddots & \vdots \\ 0 & \sigma_{MN} & \sigma_{1N} & \sigma_{1N} & \cdots & \rho_N \end{bmatrix} \quad (\text{A2})$$

Here, f is the ratio of the equilibrium populations in the M and B states, and k is the $M \rightarrow B$ exchange rate, *i.e.*, $1/k$ is the mean residence time of a nucleus in site M. The auto-relaxation rates, ρ_i , and cross-relaxation rates, σ_{ij} , of the explicitly dipole-coupled nuclei are

$$\rho_i = \sum_{\substack{j=1 \\ j \neq i}}^N \rho_{ij} \quad (\text{A3})$$

$$\rho_{ij} = D_{ij}^2 [0.1 j(0) + 0.3 j(\omega_0) + 0.6 j(2\omega_0)] \quad (\text{A4})$$

$$\sigma_{ij} = D_{ij}^2 [0.6 j(2\omega_0) - 0.1 j(0)] \quad (\text{A5})$$

with the dipole coupling constant

$$D_{ij} = \left(\frac{\mu_0}{4\pi} \right) \frac{\hbar \gamma^2}{r_{ij}^3} \quad (\text{A6})$$

If the protein dynamics can be modeled as rotational diffusion of a rigid spherical top, the spectral density function takes the simple form

$$j(\omega) = \frac{\tau_c}{1 + (\omega\tau_c)^2} \quad (\text{A7})$$

The following treatment, however, is valid also for more sophisticated spectral density functions.^{52,53}

Our aim here is to calculate the evolution of the nonequilibrium longitudinal magnetization, $\Delta I_{zB}(t)$, associated with the bulk-like environment. The formal solution to eq A1 is

$$\mathbf{X}(t) = \exp(-\mathbf{R}t)\mathbf{X}(0) \quad (\text{A8})$$

showing that $\Delta I_{zB}(t)$ decays in general as a sum of $N + 2$ exponentials. In practice, however, it is often found that the decay of $\Delta I_{zB}(t)$ is indistinguishable from a single exponential. The effective longitudinal relaxation rate, R_B , measured under such conditions can be obtained as

$$1/R_B = \int_0^\infty dt \Delta I_{zB}(t)/\Delta I_{zB}(0) \quad (\text{A9})$$

By Laplace transforming eq A8, one obtains from eq A9

$$1/R_B = (\mathbf{R}^{-1})_{BB} + (\mathbf{R}^{-1})_{BM} \Delta I_{zM}(0)/\Delta I_{zB}(0) + \sum_{i=1}^N (\mathbf{R}^{-1})_{Bi} \Delta I_{zi}(0)/\Delta I_{zB}(0) \quad (\text{A10})$$

For selective excitation of the B spins, only the first term in eq A10 contributes since then $\Delta I_{zM}(0) = \Delta I_{zi}(0) = 0$. The remaining terms can actually be neglected also in the case of nonselective excitation provided that $f \ll 1$ and $\rho_B \ll (\rho_M, \rho_1, \rho_2, \dots, \rho_N)$, as is frequently the case. For selective excitation of the macromolecular spins, however, the observed B spin magnetization obviously evolves nonmonotonically (since $\Delta I_{zB}(0) = 0$). The concept of an effective relaxation rate is therefore not useful in this case.

Taking the inverse of the rate matrix \mathbf{R} and using elementary properties of determinants, we find from eq A10 that the effectively exponential decay of the nonequilibrium bulk magnetization is governed by a relaxation rate

$$R_B = \rho_B + \frac{f}{\frac{1}{R_M} + \frac{1}{k}} \quad (\text{A11})$$

with the intrinsic relaxation rate, R_M , of the exchanging macromolecular site given by

$$R_M = \rho_M - \frac{1}{\det(\mathbf{P})} \sum_{i=1}^N \sigma_{Mi} \det(\mathbf{P}_i) \quad (\text{A12})$$

where \mathbf{P} is the relaxation matrix for the nonexchanging macromolecular spins

$$\mathbf{P} = \begin{bmatrix} \rho_1 & \sigma_{12} & \cdots & \sigma_{1N} \\ \sigma_{12} & \rho_2 & \cdots & \sigma_{2N} \\ \vdots & \vdots & \ddots & \vdots \\ \sigma_{1N} & \sigma_{2N} & \cdots & \rho_N \end{bmatrix} \quad (\text{A13})$$

and the matrix \mathbf{P}_i is obtained from \mathbf{P} by replacing the i :th row of \mathbf{P} by $(\sigma_{M1}, \sigma_{M2}, \dots, \sigma_{MN})$. For the case of selective (B spin) excitation, eqs A11–A13 represent an exact result for the effective relaxation rate R_B defined in eq A9. For nonselective excitation, the result is an accurate approximation as long as $f \ll 1$ and $\rho_B \ll R_M$. If all cross-relaxation rates σ_{Mi} vanish, then $R_M = \rho_M$ and, eq A11 reduces to the well-known⁴⁴ result for two-site exchange under the conditions $f \ll 1$ and $\rho_B \ll \rho_M$. Using eqs A3–A5, it can be shown that $\det(\mathbf{P})$ and $\sigma_{Mi} \det(\mathbf{P}_i)$ are non-negative and, hence, that the effect of the cross-relaxation rates σ_{Mi} is always to reduce the intrinsic relaxation rate R_M , *i.e.*, the inequality $R_M \leq \rho_M$ holds generally. For the special case of a rigid, spherical-top protein, with the spectral

density function as in eq A7, the cross-relaxation contribution to R_M vanishes when $\sigma_{Mi} = \sigma_{ij} = 0$, i.e., when $\omega_0\tau_c = \sqrt{5}/2$.

For $N = 1$, eq A12 reduces to

$$R_M = \rho_M - \frac{\sigma_{M1}^2}{\rho_1} \quad (\text{A14})$$

and for $N = 2$

$$R_M = \rho_M - \frac{(\rho_1\sigma_{M2}^2 + \rho_2\sigma_{M1}^2 - 2\sigma_{M1}\sigma_{M2}\sigma_{12})}{(\rho_1\rho_2 - \sigma_{12}^2)} \quad (\text{A15})$$

If the cross-relaxation rates, σ_{ij} , between the macromolecular spins are neglected, the general result, eq A12, reduces to

$$R_M = \rho_M - \sum_{i=1}^N \frac{\sigma_M^2}{\rho_i} \quad (\text{A16})$$

The preceding results are readily generalized to the case where the exchanging entity is a two-spin system, such as the protons

in a water molecule. The only difference is that now the two cross-relaxation rates that couple the exchanging and non-exchanging macromolecular spins are no longer equal; instead, we have

$$\sigma_{Mi} = \frac{1}{2}\sigma_{iM} = \sigma_{M1i} + \sigma_{M2i} \quad (\text{A17})$$

The net effect of this modification is that the cross-relaxation terms in eqs A12 and A13–A16 are multiplied by a factor 1/2. The auto-relaxation rate of the M spins is now given by

$$\rho_M = (\rho_{M1M2} + \sigma_{M1M2}) + \frac{1}{2} \sum_{i=1}^N (\rho_{M1i} + \rho_{M2i}) \quad (\text{A18})$$

while the auto-relaxation rates ρ_i of the nonexchanging spins are given by eq A3 with the summation including the two M spins.

JA963611T